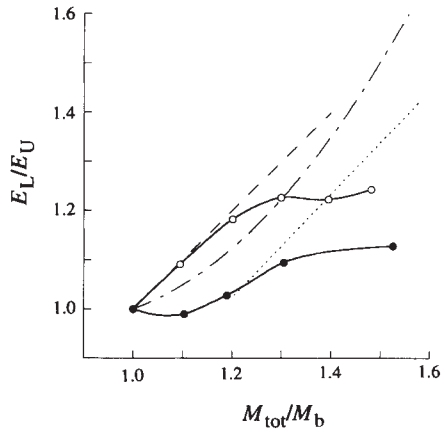

FIG. 3 The mechanical energy output and the total energy consumed when carrying loads is compared with the energy output or consumed when walking unloaded, as a function of load. The ratio of the total work done when walking with a load to the total work done when walking unloaded is shown for the African women (filled circles) and the control subjects (open circles). The dotted line is the straight line used by Maloiy *et al.*[1] to fit their Fig. 3 data of the ratio of oxygen consumption rate in African women carrying loads to their oxygen consumption rate when unloaded. Similarly, the dashed line, also from Maloiy *et al.*, is the relationship found for untrained adults carrying loads on their backs or their heads. The dot–dash line is the same ratio, calculated from Pandolf *et al.*[8], for army recruits carrying backpacks. Note that the African women can carry loads of nearly 20% of their body weight with no increase in their total work, whereas, for the same loads, the control subjects' work increases in proportion to the load. For loads greater than 30% of body weight, both the African women and the controls show little further increase in the total work, indicating that the work ratio is no longer indicative of the oxygen consumption ratio, which increases continuously with load (dotted and dashed lines). However, the work ratio of the African women at these high loads is only about half that of the controls. The work ratio on the ordinate was calculated as:

$$\frac{W_{tot,L}}{W_{tot,U}} = \frac{W_{ext,L} + 0.537W_{tot,U}}{W_{tot,U}}$$

$$= \frac{\frac{W_{ext,L}}{W_{ext,U}} 0.463W_{tot,U} + 0.537W_{tot,U}}{W_{tot,U}}$$

$$= \frac{W_{ext,L}}{W_{ext,U}} 0.463 + 0.537$$

on the assumption that the internal work, namely the work required to move the body segments relative to the combined centre of mass, is equal to the unloaded walking value (that is, $0.537W_{tot,U}$) (ref. 9); the U and L subscripts indicate unloaded and loaded measurements, respectively. The ratio $W_{ext,L}/W_{ext,U}$ was calculated for each load by multiplying the data in the bottom of Fig. 2 times the total weight (body weight plus any load).

of the control subjects (Fig. 3, dotted against dashed lines) is accounted for by the finding that the increment in W_{tot} by the African women is much less than that done by the controls at all loads.

The dissociation between the increase in energy expenditure and the increase in mechanical work for loads greater than 30% of body weight may be due to factors not measured here as mechanical work, but which nevertheless increase the energy expenditure at these high loads. These factors may include a decrease in muscular efficiency, an increase in isometric contractions required to maintain posture and support the load, and increase in the internal work due to movements of the load relative to the centre of mass. Alternatively, the skill of these women in carrying head-supported loads may require muscular strength appropriate for the load. At very high loads in the African women, and at all loads in the control subjects, the required strength may not be available; this may also help explain the finding that obese African women do not exhibit the same economy of head-supported load carriage[4].

In conclusion, African women can carry head-supported loads of up to 20% of their body weight for 'free', because their total mechanical work of walking does not increase. Furthermore, they carry loads of up to 70% of their body weight for a lower metabolic cost than control subjects carrying either head- or back-supported loads because they do less mechanical work. They conserve more mechanical energy through a more complete energy transfer, back and forth between the kinetic energy of forward motion and the potential energy of their centre of mass; in effect, they become better pendulums. □

Received 26 September 1994; accepted 24 February 1995.

1. Maloiy, G. M. O., Heglund, N. C., Prager, L. M., Cavagna, G. A. & Taylor, C. R. *Nature* **319,** 668–669 (1986).
2. Alexander, R. McN. *Nature* **319,** 623–624 (1986).
3. Alexander, R. McN. *Elastic Mechanisms in Animal Movement* 95–97 (Cambridge Univ. Press, 1988).
4. Jones, C. D. R., Jarjou, M. S., Whitehead, R. G. & Jequier, E. *Lancet* **XII,** 1331–1332 (1987).
5. Cavagna, G. A. *J. appl. Physiol.* **39,** 174–179 (1975).
6. Cavagna, G. A., Thys, H. & Zamboni, A. *J. Physiol., Lond.* **262,** 639–657 (1976).
7. Heglund, N. C. *J. exp. Biol.* **93,** 333–338 (1981).
8. Pandolf, K. B., Givoni, B. & Goldman, R. F. *J. appl. Physiol.* **43**(4), 577–581 (1977).
9. Willems, P. A., Cavagna, G. A. & Heglund, N. C. *J. exp. Biol.* **198,** 379–393 (1995).

ACKNOWLEDGEMENTS. This study was supported by the US Fulbright Scholar Program, the US Army Research Office, the Belgian FNRS, and the Italian MURST. We thank the University of Nairobi, the Concord Field Station of Harvard University, and J. D. Harry for their facilities, equipment and assistance.

Use of implicit motor imagery for visual shape discrimination as revealed by PET

Lawrence M. Parsons*†, Peter T. Fox*, J. Hunter Downs*, Thomas Glass*, Traci B. Hirsch*, Charles C. Martin*, Paul A. Jerabek* & Jack L. Lancaster*

* Research Imaging Center, University of Texas Health Science Center at San Antonio, 7703 Floyd Curl Drive, San Antonio, Texas 78284-6240, USA
† Department of Psychology, University of Texas at Austin, Austin, Texas 78712, USA

POSITRON emission tomography (PET) can be used to map brain regions that are active when a visual object (for example, a hand) is discriminated from its mirror form. Chronometric studies[1–3] suggest that viewers 'solve' this visual shape task by mentally modelling it as a reaching task, implicitly moving their left hand into the orientation of any left-hand stimulus (and conversely for a right-hand stimulus). Here we describe an experiment in which visual and somatic processing are dissociated by presenting right hands to the left visual field and vice versa. Frontal (motor), parietal (somatosensory) and cerebellar (sensorimotor) regions similar to those activated by actual[4,5] and imagined[6–8] movement are strongly activated, whereas primary somatosensory and motor cortices are not. We conclude that mental imagery is realized at intermediate-to-high order, modality-specific cortical systems, but does not require primary cortex and is not constrained to the perceptual systems of the presented stimuli.

Virtually all brain regions known to participate in the planning and execution of bodily movements (with the exception of primary sensorimotor cortex, see later) were activated

TABLE 1 Activation foci

Plot	Area	Extent (mm^3)	Intensity (c.b.f. change)	Z-score	P	Coordinate x mm	y mm	z mm
Left hands, right visual field								
3	BA6	504	5	3.1	**	−6	1	60
9R	BA40	584	6	3.5	****	38	−38	50
8L	BA7	752	5	2.8	**	−30	−60	50
4R	BA6	544	5	2.8	**	26	−2	48
4L	BA6	840	7	3.7	*****	−26	−12	48
8R	BA7	688	5	2.8	**	34	−54	48
8R	BA7	600	5	2.7	**	28	−64	46
8L	BA7	536	5	2.9	**	−20	−64	46
7L	BA6	784	7	3.9	*****	−2	16	46
4L	BA6	648	5	3.1	**	−40	−8	46
8L	BA7/40/19	416	5	2.8	**	−34	−66	42
9L	BA40	80	5	2.6	**	−32	−58	40
9R	BA40	536	5	2.6	**	38	−56	38
9L	BA40	992	6	3.5	****	−36	−42	38
5R	BA44	656	6	3.4	***	42	4	34
5L	BA44	672	5	2.9	**	−44	0	32
2	BA46/9	400	5	2.8	**	36	32	26
6R	INS	496	5	3.1	**	27	20	6
13L	CBM	368	6	3.4	***	−6	−44	−6
19R	CBM	632	5	2.9	**	38	−73	−16
19L	CBM	872	6	3.4	***	−8	−76	−16
13R	CBM	760	7	4.0	*****	46	−65	−18
13L	CBM	512	6	3.1	**	−38	−52	−18
13L	CBM	360	5	2.8	**	−10	−36	−20
19L	CBM	216	5	2.7	***	−51	−76	−24
13R	CBM	328	5	2.8	**	17	−48	−28
13R	CBM	352	5	2.6	**	40	−48	−30
13R	CBM	392	5	2.8	**	32	−38	−32
13R	CBM	352	5	2.6	**	24	−62	−36

Plot	Area	Extent (mm^3)	Intensity (c.b.f. change)	Z-score	P	Coordinate x mm	y mm	z mm
Right hands, left visual field								
3	BA6	72	5	2.7	**	−4	−2	59
4R	BA6	160	5	2.9	**	32	−10	54
3	BA6	168	5	2.6	**	−5	8	54
4L	BA6	568	6	3.3	***	−26	−10	54
4R	BA6	160	5	2.8	**	26	−2	54
8L	BA7	584	6	3.4	****	−30	−58	52
8R	BA7	152	5	3.1	**	22	−48	48
8L	BA7	160	5	2.9	**	−19	−62	46
4L	BA6	456	6	3.6	***	−38	−6	46
8R	BA7	344	6	3.3	***	26	−56	46
7L	BA6	208	6	3.5	****	−4	16	44
8R	BA7	128	5	2.9	**	16	−66	42
9L	BA40	536	6	3.5	****	−42	−40	42
9L	BA40	536	6	3.2	***	−34	−40	42
9R	BA40	272	5	3.0	**	42	−30	40
8R	BA7	400	7	3.8	*****	27	−38	36
5L	BA44/6	96	5	2.7	**	−46	−1	32
2	BA46/9	80	5	2.8	**	−45	36	30
5L	BA44	88	5	2.7	**	−60	14	16
6L	INS	32	5	2.6	**	−32	12	14
5R	BA44/45	112	6	3.4	****	56	24	12
19R	CBM	136	5	2.9	**	14	−67	−8
13L	CBM	104	5	2.8	**	−8	−44	−9
13R	CBM	112	5	3.0	**	20	−51	−14
13L	CBM	176	6	3.2	***	−11	−46	−14
19R	CBM	272	5	3.1	**	42	−72	−22
19L	CBM	80	5	3.0	**	−52	−76	−24
19R	CBM	64	5	2.7	**	10	−70	−24
19R	CBM	24	5	2.6	**	2	−80	−26
19R	CBM	224	6	3.4	****	30	−68	−28
13R	CBM	40	5	2.6	**	18	−48	−28
19L	CBM	32	5	2.7	**	−10	−79	−32

Focal increases in brain blood flow in somatic sensory and motor areas occurring during each experimental condition (relative to rest) are listed. (A comprehensive listing of all brain areas active in these tasks is available in the BrainMap database or as Supplementary Information from *Nature*.) 'Plot' identifies the regional activation into which the focus was clustered (Fig. 2). 'Area' indicates the anatomic structure(s) activated by Brodmann area (BA) or structure name (INS, insula; CBM, cerebellum). 'Extent' is the total volume of all contiguous pixels above statistical threshold ($P < 0.005$) of each focus. 'Intensity' is the peak change in cerebral blood flow (c.b.f.; expressed in millilitres per 100 g per min) occurring within the activated site. 'Z-score' is intensity divided by image noise. '*P*' is statistical significance: *, 0.005; **, 0.001; ***, 0.0005; ****, 0.0001; *****, 0.00005 (ref. 29). 'Coordinates' are expressed in mm from the anterior commissure: *x*, right(+)/left(−); *y*, anterior(+)/posterior(−); *z*, superior(+)/inferior(−). Coordinate and area follow ref. 30.

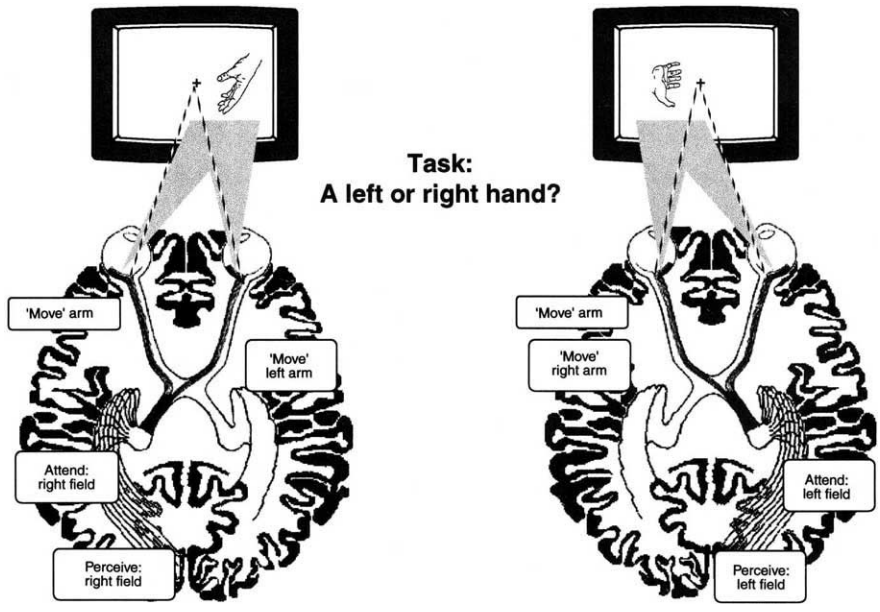

FIG. 1 Experimental concept. We hypothesized that left–right judgements of visually presented hands would elicit an implicit movement of the hand corresponding to the stimulus. Hemifield-based processes were dissociated from hemisoma-based processes using the principle of cerebral contralaterality. Left hands were presented predominantly to the right visual field; right hands were presented predominantly to the left visual field. Attention to one hemifield (for example, 'attend right field') and processing visual information from that hemifield (for example, 'see right field') were expected to activate the contralateral parietal and occipital areas. Implicit movement was expected to activate the dominant (left) frontal lobe, for higher-level, less specified planning (for example, 'move' arm) and in the hemisphere contralateral to the limb 'moved' for lower-level, more specified planning (for example, 'move' left arm).

METHODS. Subjects made a covert decision as to whether a visual stimulus was a left or right hand. Subjects fixated on a black dot in the centre of a video monitor as stimuli appeared singly either in the left or right visual hemifield. They were unable to see their own hands and were not allowed to make actual movements. Physically adopting the posture of the presented hand in many instances would require coordinated activity at more than one arm joint, motion near extremes of joint limits, uncomfortable kinaesthetic sensations, and long trajectories[3]. There were two experimental tasks: a left-visual-field task and a right-visual-field task. In the left-field task, 80% of the stimuli were right hands, 20% were left hands. In the right field task, the ratios were reversed. Stimuli were presented at a mean eccentricity of 3.2°, with the edges of the stimulus 0.6° (inner edge) and 5.6° (outer edge) from fixation. Stimuli were presented for 150 ms. The time between the offset of one stimulus and onset of the next was adjusted to allow just barely enough time for task performance, based on prior chronometric pilots. These conditions, allowing no time for introspection, heightened the implicit nature of the performance. The rest condition was fixation on the central dot.

by this visual shape task (Figs 1 and 2; Table 1). Prefrontal and insular premotor areas (clusters 2, 6), involved in global spatial and temporal schemata for movement preparation[4,9], were purely contralateral to stimulus handedness (somatic laterality). Supplementary motor area (SMA, cluster 3), active during imagined movement[6,7] and important in motor memory and sequencing[9,10], was strongly activated in left brain for both conditions, reflecting cerebral dominance for motor programming (dominance laterality). Anterior cingulate, in a region probably projecting onto SMA[10], showed dominance laterality. Superior premotor cortex (Brodmann area (BA) 6, cluster 4) activated bilaterally but more strongly in the left hemisphere, a motor-dominance laterality. Inferior premotor cortex (BA44/45, cluster 5) activated bilaterally with somatic laterality. Superior and inferior premotor areas are important for planning, initiation, guidance and execution of simple and skilled motor tasks and limb movements in extrapersonal space[11–13]. Cerebellum and basal ganglia (clusters 13, 19), known to be active during actual movement[5,11], were bilaterally active. No activation was detected in primary somatic sensory or primary motor cortex, consistent with the absence of body movement during the task.

Posterior and inferior parietal cortex—multimodal association areas important to body schema, egocentric space and action planning[14–16]—activated bilaterally but showed a mix of visual, somatic and dominance lateralizations. For both conditions, superior parietal regions (BA7) were active bilaterally, with somewhat more activation in the hemisphere contralateral to stimulus hemifield (cluster 8, Fig. 2). We interpret this as a posterior attentional system aiding covert shifts of attention to the contralateral hemifield[17]. Inferior parietal (BA40) was bilaterally active with a hand effect stronger for right hands than for left (cluster 9, Fig. 2).

These somatic-motor activations support the principle that mental imagery is realized using modality-specific neural systems. This is most frequently hypothesized in the perceptual domain[18]. Namely, visual systems subserve visual imagery; auditory systems subserve auditory imagery. Our motor-system activations reflect implicit motor imagery (as argued below). These data confirm and considerably extend preliminary indications of correspondence between the neural systems for actual and imagined movement[6–8]. Note that motor imagery was realized through neural systems of movement but did not require the primary sensory or motor cortices, perhaps unlike visual imagery[18]. In addition, these data confirm the hypothesis[1,3] that motor imagery can be employed to solve problems posed in perceptual domains, using mental transformations of the viewer rather than of the viewed object. This supports the principle

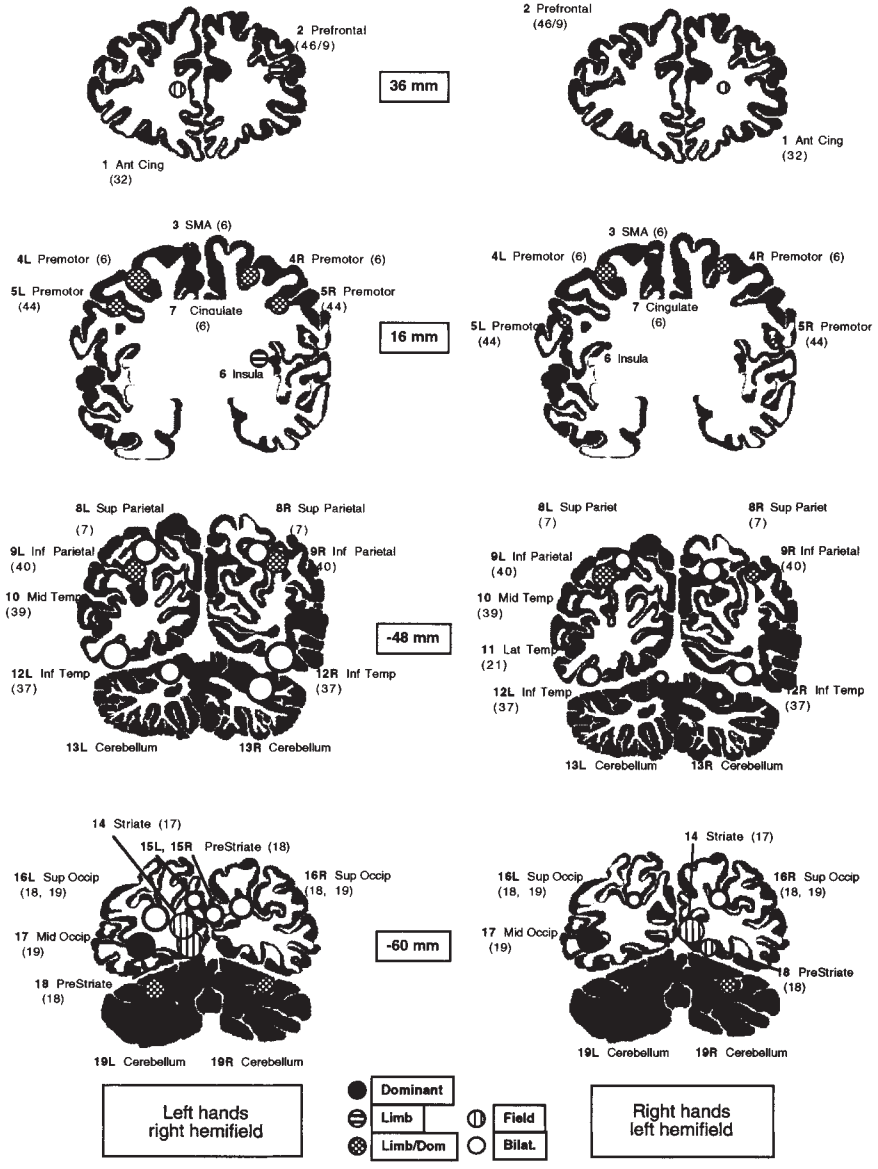

FIG. 2 Activation cluster plot. Each circle designates a cluster of focal, task-induced increases in cerebral blood flow ($P < 0.005$). Circles depict the mean location and collective extent of one or more discrete foci (Table 1). Brain contours are coronal sections positioned +36 mm, +16 mm, −48 mm, and −60 mm from the anterior commissure. Probable Brodmann cytoarchitectonic areas are given parenthetically.

METHODS. Discrete activation foci (Table 1) were grouped into regional-activation clusters based upon probable Brodmann area and gyrus (Table 1). Clusters are represented as circles. The circle representing each cluster is centred on the mean location for all local maxima included in the cluster. The area of each plotted circle is an accurate 2D projection of the sphere—true to the scale of the section—whose volume equals the sum of the activated voxels of the clustered foci. Each voxel had a volume of 8 mm^3. Clusters are plotted on the nearest coronal section.

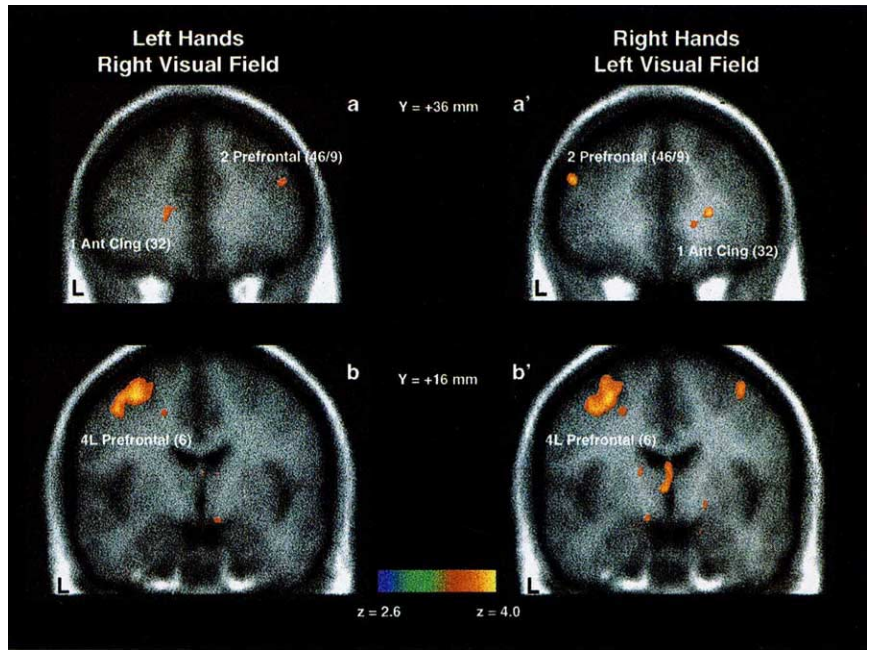

FIG. 3 PET/MRI superposition. Three types of hemispheric lateralization are illustrated: field effect, hand effect and dominance effect. The anterior cingulate (Ant Cing) remains contralateral to the visual field of the stimulus, a field effect (a, a'). Prefrontal cortex remains contralateral to the body-side requiring implicit movement, a hand effect (a, a'). Premotor cortex is stronger in the motorically dominant hemisphere (left hemisphere in our right-handed population), regardless of the visual field or body side of the stimulus, a dominance effect (b, b'). Images were formed by superposition of the averaged (grand mean) PET functional data (colour) onto the averaged (grand mean) MRI anatomical data (grey scale). PET data are *z*-scores (Table 1) displayed on a colour scale ranging from 2.6 (blue; $P<0.005$) to 4.0 (yellow; $P<0.00003$). Images are coronal sections positioned +36 mm (a and a'), and +16 mm (b and b') in front of the anterior commissure. Probable Brodmann cytoarchitectonic areas are given in parentheses.

METHODS. The subjects were seven, healthy right-handed normal volunteers (six men and one woman, ranging in age from 20 to 35 yr, with a mean of 24 yr). After giving informed consent, each subject underwent nine PET blood-flow scans, three in each experimental task and three in fixation-point rest. Images were averaged within condition for each subject. Images were spatially normalized into the bicommissural coordinate space[29] and then averaged within condition among subjects. The grand-mean image for each task was compared to control, forming grand-mean images of the task-induced changes in brain activity. Grand-mean images were converted to *z*-score images using the population variance[29]. To ensure that each subject performed the task as requested, an experiment was performed at the conclusion of the scanning session. In the post task, a hand was presented in central fovea until the subject pressed a left or right button to indicate whether it was a left or right hand[1–3]. Subjects were fast and accurate overall and faster for the stimuli from the experiment than for other stimuli, thus exhibiting general and stimulus-specific practice effects of their implicit performance in the experiment.

that abstract reasoning relies on physical analogies, employing mental models of physical objects and actions[12,19].

Visual processing areas were highly active. Primary (BA17, cluster 14) and early extraprimary (BA18, cluster 18) responses were purely contralateral to visual field (visual laterality). Some superior occipital responses (BA18/19, cluster 16) showed weak visual laterality, or were bilateral (BA18, cluster 15). Inferior temporal cortex (BA37, cluster 12), involved in representing object-based information[20,21], activated bilaterally, reflecting its bilateral receptive fields[22]. Lateral, inferior occipital cortex (BA19, cluster 17) activated solely on the left in both conditions. This strongly supports prior observations indicating a specific role in assembling visual percepts and images for this left-sided region[23]. Two regions in anterior cingulate, one rostral (BA32, cluster 1) and one inferior (BA24, 25; LH15, RH50, Table 1) also showed visual laterality. These probably reflect covert shifts of attention to the hemifield of the stimulus[17].

Visual recognition of objects is an active process whereby visual percepts are mapped onto stored mental representations[24]. When viewing objects at unfamiliar orientations, the recognition process is sometimes enabled by mentally reorienting the object[25,26]. For example, identity judgments of pairs of similarly shaped but dissimilarly oriented objects require the imagined rotation of one object to the orientation of the other[27]. That the time required for such operations is an approximately linear function of rotation angle is a finding now considered classical in cognitive science. Such results demonstrate that imagined spatial transformations of abstract shapes often are performed in a viewer-based or scene-based visual space[28]. Our results and the chronometric studies[1–3] upon which our study was predicated demonstrate that this is not always the case.

Response times for handedness judgements of visually presented body parts are far better modelled in a somatic space—a biomechanical joint space—than in a visual space. Specifically, chronometry suggests that a somatic representation is moved from the observer's current body position to the stimulus' orientation without violating joint constraints[1–3]. In fact, the time required for this visual discrimination is proportional to that of actual movement[3]. We interpret this as the execution of an implicit movement, as actual movements do not occur, imagined movements are not requested, and subjects often are unaware of an imagined movement (Fig. 1 legend).

The experimental strategy used here is noteworthy. Typically, PET studies strive for reductionism, contrasting conditions that (putatively) differ by a single cognitive operation. Here we distinguished somatic from visual operations by exploiting known differences in lateralization (retinotopic versus somatotopic), rather than by a reductionist design. Although such paradigms have been used for chronometric studies of split-brain patients, this is their first adaptation to functional neuroimaging. As our two tasks were complementary, rather than reductionist, each was contrasted with (subtracted from) a neutral control state (Figs 1 and 3 legends). Comparison to a neutral baseline allows all brain areas participating in a task to be localized and lateralized, protecting against the effects of incorrect *a priori* judgements about the number and nature of cognitive operations (Donders' fallacy)[23]. Such caution is advisable when exploring new paradigms and mental operations.

Choice of an experimental design based on differences in lateralization assumed that subjects would implicitly move only the correct hand. That is, the mental representation of their right hand is moved when presented with a right hand and vice versa. Prior chronometric studies[1–3] indicate that pre-attentive recognition of the presented hand's laterality is followed by a confirmatory implicit movement of the correct hand, which allows an explicit judgement of the handedness of the stimulus.

An unexpected, unprecedented but very robust finding was that right-field stimuli induced much more extensive (178%, on average) activations than did left-field stimuli. This was true for responses in both hemispheres. However, the intensity and number of foci in corresponding regions did not differ. This was true for all active regions except primary visual cortex (BA17),

which argues that the effect was not an artefact of apparatus or method. This observation implies that processing of information from the dominant (right) visual field is more extensive than that of information from the non-dominant (left) visual field, irrespective of the hemisphere or region within which this processing is realized. □

Received 16 September 1994; accepted 21 February 1995.

1. Parsons, L. M. *Cogn. Psych.* **19,** 178–241 (1987).
2. Parsons, L. M. *J. exp. Psych.* **116,** 172–191 (1987).
3. Parsons, L. M. *J. exp. Psych.* **20,** 709–730 (1994).
4. Frith, C. D., Friston, K., Liddle, P. F. & Frackowiak, R. S. J. *Proc. R. Soc.* **244,** 241–246 (1991).
5. Roland, P. E., Meyer, E., Shibasaki, Y. L., Yamamoto, Y. L. & Thompson, C. J. *J. Neurophysiol.* **48,** 467–480 (1982).
6. Roland, P. E., Lassen, N. A., Larsen, B. & Skinhoj, E. *J. Neurophysiol.* **43,** 118–136 (1980).
7. Fox, P. T., Pardo, J. V., Petersen, S. E. & Raichle, M. E. *Soc. Neurosci. Abstr.* **13,** 1433 (1987).
8. Decety, J. *et al. Nature* **371,** 600–602 (1994).
9. Goldberg, M. J. & Bruce, C. J. *J. Neurophysiol.* **64,** 489–508 (1990).
10. Tanji, J. *Neurosci. Res.* **19,** 251–268 (1994).
11. Posner, M. I. & Petersen, S. E. *A. Rev. Neurosci.* **13,** 25–42 (1990).
12. Colebatch, J. G., Deiber, M. P., Passingham, R. E., Friston, K. S. & Frackowiak, R. S. J. *J. Neurophysiol.* **65,** 1392–1401 (1991).
13. Dum, R. P. & Strick, P. L. in *Motor Control: Concepts and Issues* (eds Humphrey, D. R. & Freund, H.-J.) 383–397 (Wiley, New York, 1991).
14. Andersen, R. A. in *Handbook of Physiology* (eds Plum, F. & Mountcastle, V. B.) 483–518 (Am. Physiol. Soc., Bethesda, Maryland, 1987).
15. Heilman, K. M., Watson, R. T. & Valenstein, E. in *Clinical Neuropsychology* (eds Heilman, K. M. & Valenstein, E.) 279–336 (Oxford University Press, New York, 1993).
16. Stein, J. F. in *The Brain and Space* (ed. Paillard, J.) 185–222 (Oxford University Press, New York, 1991).
17. Heilman, K. M. & Rothi, L. J. in *Clinical Neuropsychology* (eds Heilman, K. M. & Valenstein, E.) 141–163 (Oxford University Press, New York, 1993).
18. Kosslyn, S. M. *et al. J. Cogn. Neurosci.* **5,** 263–287 (1993).
19. Johnson-Laird, P. N. in *Foundations of Cognitive Science* (ed. Posner, M. I.) 469–499 (MIT Press, Cambridge, Massachusetts, 1989).
20. Ungerleider, L. G. & Mishkin, M. in *Analysis of Visual Behavior* (eds Ingle, D. J., Goodale, M. A. & Mansfield, R. J. W.) 549–586 (MIT Press, Cambridge, Massachusetts, 1982).
21. Perrett, D. I., Oram, M. W., Hietanen, J. K. & Benson, P. J. in *Neuropsychology of Higher Level Vision* (eds Farah, M. & Ratcliff, R.) 33–61 (MIT Press, Cambridge, Massachusetts, 1994).
22. Gross, C. G., Rocha-Miranda, C. E. & Bender, D. B. *J. Neurophysiol.* **35,** 96–111 (1972).
23. Posner, M. I. & Raichle, M. E. *Images of Mind* 30–31, 90–95 (Freeman, New York, 1994).
24. Biederman, I. in *Invitation to Cognitive Science II* (eds Osherson, D., Kosslyn, S. M. & Hollerbach, J. M.) 41–72 (MIT Press, Cambridge, Massachusetts, 1990).
25. Tarr, M. J. *Psychonom. Bull. Rev.* **2,** 55–82 (1995).
26. Marr, D. *Vision* (Freeman, San Francisco, 1982).
27. Shepard, R. N. & Cooper, L. *Mental Images and their Transformations.* (MIT Press, Cambridge, Massachusetts, 1982).
28. Hinton, G. E. & Parsons, L. M. *Cognition* **30,** 1–35 (1988).
29. Fox, P. T. & Mintun, M. A. *J. nucl. Med.* **30,** 141–149 (1989).
30. Talairach, J. & Toumoux, P. *Co-planar Stereotaxic Atlas of the Human Brain* (Thieme Medical, New York, 1988).

SUPPLEMENTARY INFORMATION. Enquiries should be addressed to Mary Sheehan at the London office of *Nature*.

ACKNOWLEDGEMENTS. Supported by grants from the EJLB Foundation and the Research Imaging Center. We thank J. Gabrieli, M. Posner and L. Ungerleider for their comments. Data reported here are available through the BrainMap Database (bmap.admin@uthscsa.edu).

Homeotic genes and the regulation and evolution of insect wing number

Sean B. Carroll, Scott D. Weatherbee & James A. Langeland

Howard Hughes Medical Institute and University of Wisconsin-Madison, 1525 Linden Drive, Madison, Wisconsin 53706, USA

THE evolution of wings catalysed the radiation of insects which make up some 75 per cent of known animals. Fossil evidence suggests that wings evolved from a segment of the leg[1] and that early pterygotes bore wings on all thoracic and abdominal segments[2]. The pterygote body plan subsequently diverged producing orders bearing three, two or just one pair of thoracic wings. We have investigated the role of homeotic genes in pterygote evolution by examining their function in *Drosophila* wing development and their expression in a primitive apterygote. Wing formation is not promoted by any homeotic gene, but is repressed in different segments by different homeotic genes. We suggest here that wings first arose without any homeotic gene involvement in an ancestor with a homeotic 'groundplan' similar to modern winged insects and that wing formation subsequently fell under the negative control of individual homeotic genes at different stages of pterygote evolution.

The *Drosophila* wing and haltere primordia can first be visualized as discrete clusters of *vestigial*-expressing (Fig. 1*a*) and *snail*-expressing[3] (Fig. 1*b*) cells in the second and third thoracic segments of the stage 12 embryo. Antibodies specific for the *vestigial* and *snail* proteins serve as interchangeable markers for the flight appendage primordia because they label the same cells at different embryonic stages (Fig. 1*c–h*). Both genes have a role in formation of the flight appendages because *vestigial* mutants lack wings and halteres[4] and weak *snail* mutants that survive to adulthood exhibit a hemithorax or missing haltere phenotype[5].

The restriction of the flight appendage primordia to the two posterior thoracic segments of the *Drosophila* embryo suggests a role for homeotic genes in specifying which segments will bear wings. Because the *Antennapedia* (*Antp*) gene is expressed in the second and third thoracic segments during embryogenesis[6,7], this gene might regulate the formation of the wing and haltere primordia. Surprisingly, there is no requirement for *Antp* gene function during the formation of these primordia (Fig. 1*i*). This suggests that wing primordium formation as it occurs in the mesothoracic (T2) segment represents a 'ground state' of embryonic development without the input of the homeotic genes. Furthermore, this indicates that ectopic wing primordia found in other homeotic mutants (see below) result from derepression of the wing developmental programme, rather than the derepression of *Antp*.

It appears that, rather than *Antp* positively regulating wing and haltere formation in T2 and T3, other homeotic genes repress the wing primordia in different body segments. For example, the *Sex combs reduced* (*Scr*) gene is expressed in the labial and prothoracic (T1) segment[8,9]. In *Scr* mutant embryos ectopic flight appendage primordia arise in the T1 segment, demonstrating that *Scr* normally represses wing formation there (Fig. 1*j*). Similarly, in mutants for the *Ultrabithorax* (*Ubx*) gene, which normally functions in both the metathoracic (T3) and first abdominal segment (A1)[10], the haltere primordia in T3 expands to the size of the wing primordia (data not shown) and an ectopic primordium forms in the ventral region of A1 (Fig. 1*k*). The potential for wing formation exists in most or all trunk segments as illustrated by embryos lacking the *abd-A* gene (Fig. 1*l*) or the *Ubx* and *abdominal-A* (*abd-A*) genes (Fig. 1*m*) (see also ref. 11).

The experiments above address only the formation of the embryonic wing primordia and not the growth and development of adult wings from these primordia. Cells may respond differently to the expression of a particular homeotic gene at different stages of development[12]; thus *Antp* could function during later stages of wing formation. There are no genetic requirements for *Antp*, *Scr* and *Ubx* in the formation of adult wings (*Antp* is required in the mesonotum)[13]. Furthermore, we find that *Antp* protein expression is largely absent from the region of the growing third instar imaginal disc that will give rise to the wing itself (Fig. 2*a*, *b*), again illustrating that this appendage forms without homeotic input.

To test whether the absence of *Antp* was important for wing formation, we examined wing discs in which *Antp* was ectopically expressed using the GAL4-UAS system[14]. Ectopic *Antp* expression had no effect on wing disc morphology or *vestigial* expression (not shown). Similarly, we examined the impact of *Scr* expression, which is normally absent from the wing disc, upon wing development. We find that wing development is sensitive to *Scr* repression in the embryo, but not at later stages. For instance, when *Scr* expression is driven ectopically in the growing wing disc, there is no apparent effect on wing formation as indi-